

# Calcium phosphate biocement using bone meal and acid urease: An eco-friendly approach for soil improvement

Sivakumar Gowthaman<sup>a,\*</sup>, Moeka Yamamoto<sup>b</sup>, Kazunori Nakashima<sup>a</sup>, Volodymyr Ivanov<sup>c</sup>, Satoru Kawasaki<sup>a</sup>

<sup>a</sup> Division of Sustainable Resources Engineering, Faculty of Engineering, Hokkaido University, Kita 13, Nishi 8, Kita-Ku, Sapporo, 060-8628, Japan

<sup>b</sup> Department of Socio-Environmental Engineering, School of Engineering, Hokkaido University, Kita 13, Nishi 8, Kita-Ku, Sapporo, 060-8628, Japan

<sup>c</sup> Advanced Research Lab, National University of Food Technologies, 68 Volodymyrska Street, Kyiv, 01601, Ukraine

## ARTICLE INFO

Handling editor: Zhen Leng

### Keywords:

Biocementation  
Calcium phosphate  
Bone meal  
Urea hydrolysis  
Acid urease

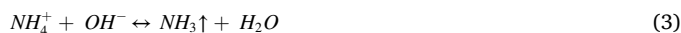
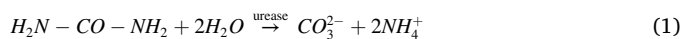
## ABSTRACT

Biocementation technology has recently become a new soil improvement method. In majority of the biocementation processes, the formation of calcium carbonate occurs as the consequence of enzymatic urea hydrolysis, producing carbonate-ions and alkaline pH (ranging between 8.5–9.5). The problem of conventional biocementation method at alkaline conditions is the release of ammonium ions (that pollute water) and gaseous ammonia (that pollutes atmosphere). In this paper, a new biocementation method is proposed, which involves calcium phosphate precipitation driven by enzymatic hydrolysis of urea. The bone meal, one of the potential and low-cost sources of calcium phosphate, was acid-dissolved and injected into the sand altogether with urea and acid urease. Due to the enzymatic hydrolysis of urea, the pH of the reaction medium increased, hence the calcium phosphate was tended to precipitate within the pores and bind the soil particles. The content of urea was varied in biocement solution to control the increase of pH during reaction, thus the biocementation was in different pH ranges. The precipitated calcium phosphate compound was found to be brushite, but its morphology highly varied depending on the pH conditions. Molar calcium/urea ratio of 1.5 in calcium phosphate biocementation solution resulted in preferable formation of plate-like crystals within the sand matrix and increased unconfined compressive strength up to 1.5 MPa. Meanwhile, the conventional biocementation is performed at molar calcium/urea ratio from 0.66 to 1.0. The calcium phosphate biocementation at pH changing from 3.4 to 7.5 indicated the potential decrease of ammonium ions release to environment by about 50% and the emission of toxic gaseous ammonia by approximately 90% in comparison with conventional biocementation.

## 1. Introduction

Biocementation is a newly emerging technology for soil improvement. Among various biocementation processes, microbially- or enzymatically induced carbonate precipitation (MICP/EICP) is gaining increased attention among geotechnical and environmental engineers (Achal et al., 2015; Almajed et al., 2020; DeJong et al., 2010; Ivanov and Stabnikov, 2017; Naveed et al., 2020). Major advantage of biocement over conventional cement is low viscosity of biocementing solution that allows its penetration into the fine pores and microchannels of the soil, and microcracks of rocks and concrete. During the conventional biocementation, the urease-producing bacteria or enzyme urease altogether with calcium salt and urea are introduced through the soil surface or injected into soil (Cheng et al., 2016; van Paassen et al., 2010). The

bacteria or enzymes facilitate the breakdown of urea into ammonium ( $\text{NH}_4^+$ ) and carbonate ions ( $\text{CO}_3^{2-}$ ) as shown in Eq. (1). In the meantime, the  $\text{CO}_3^{2-}$  reacts with available calcium ions ( $\text{Ca}^{2+}$ ) to form calcium carbonate (Eq. (2)). The calcium carbonate crystals that precipitated in soil pores enables the cementing bonds between the soil particles.



Despite the increased interests in MICP/EICP technology and several hundreds of biocement-related papers that are published annually

\* Corresponding author.

E-mail address: [gowtham1012@outlook.com](mailto:gowtham1012@outlook.com) (S. Gowthaman).

<https://doi.org/10.1016/j.jclepro.2021.128782>

Received 17 February 2021; Received in revised form 11 July 2021; Accepted 21 August 2021

Available online 22 August 2021

0959-6526/© 2021 The Authors. Published by Elsevier Ltd. This is an open access article under the CC BY license (<http://creativecommons.org/licenses/by/4.0/>).

(Omeregie et al., 2020), only few large-scale applications were reported thus far. One of the reasons is due to the environment hurdle associated with the release of harmful ammonia gas to the atmosphere, as well as the release of ammonium ions to ground/surface water (Gowthaman et al., 2020; Ivanov et al., 2019a). During the conventional MICP/EICP, hydrolysis of urea elevated the pH to 8.5–9.5, which creates the condition for calcium carbonate precipitation. In the meantime, this pH increase shifts the speciation of ammonium/ammonia, shown in Eq. (3), towards the release of toxic ammonia gas to atmosphere. In particular, the nitrogen occurs completely (~99%) in the form of ammonium ions ( $\text{NH}_4^+$ ) at  $\text{pH} \leq 7.3$ , and when pH exceeds 7.5, the equilibrium is drastically shifted to the speciation of gaseous  $\text{NH}_3$  (Whiffin, 2004). In fact, it is more controllable if the ammonium exists in the ionic form rather than the gaseous form. At post-treatment, the solution containing ammonium ions can be extracted and/or treated appropriately to avoid contaminations with ground water. The addition of zeolite (Keykha et al., 2019), or electro-biocementation (Keykha and Asadi, 2017), precipitating  $\text{NH}_4^+$  as struvite (Mohsenzadeh et al., 2021; Yu et al., 2020), and rinsing technique (Lee et al., 2019) were proposed for eliminating aqueous  $\text{NH}_4^+$  ions remaining in biocemented soils. It is worth to note, however, the emphasis given on eliminating the formation of gaseous ammonia is limited in the existing biocement methods, thus, there continues to be a need for amending existing processes or new alternative approaches for soil improvement.

In search of alternatives, calcium phosphate-based biocementation has newly been demonstrated as an eco-friendly direction, which has high potential to minimize the release of toxic ammonia gas to the atmosphere (Ivanov et al., 2019a). Calcium phosphate, similar to the calcium carbonate, is a promising engineering material with adequate strength characteristics. As listed below, there are several other merits in using calcium phosphate compounds (CPCs) for ground improvement purpose.

- CPCs are non-toxic and environmentally friendly materials (Kohn et al., 2002). CPCs are the main constituents of the bones and teeth of vertebrates, including most human hard tissues (Toshima et al., 2014), revealing that they are within the realms of possibility for establishing into the ground.
- The solubility of CPCs (presented in Fig. 1) is dependent on the pH of the surrounding environment (Kawasaki and Akiyama, 2013a; Tung, 1998). This elucidates that the acidic solution consisting of calcium and phosphate can produce insoluble CPCs when the pH of the

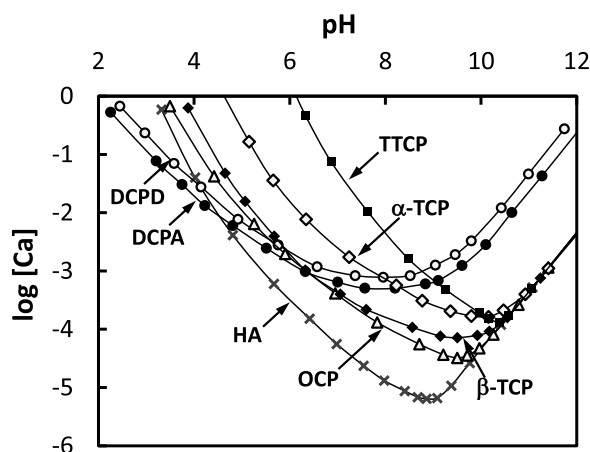


Fig. 1. Solubility isotherms of calcium phosphate compounds (DCPD is dicalcium phosphate dihydrate or brushite. DCPA is dicalcium phosphate anhydrous. OCP is octa calcium phosphate.  $\alpha$  and  $\beta$ -TCP are  $\alpha$  and  $\beta$ -tricalcium phosphates, respectively. TTCP is tetra calcium phosphate. HA is hydroxyapatite.) [Reproduced from Akiyama and Kawasaki (2012)].

medium is subjected to an increase. In addition, owing to its self-setting mechanism, the CPCs gradually undergo strengthening over the time (Ginebra et al., 1997).

- Once the treated ground is re-excavated, the CPCs can possibly be recovered from the soil as agricultural fertilizer, unlike the Portland cement (Akiyama and Kawasaki, 2012).

The development of CPC grout that can readily precipitate and cement the soil particles, was greatly challenging for engineering applications. Initially, researchers attempted to mix diammonium phosphate and calcium acetate solutions with the sand to induce the formation of CPCs, and sometimes, other additives were also incorporated to increase the mechanical strength (Akiyama and Kawasaki, 2012; Kawasaki and Akiyama, 2013a, 2013b). One major obstacle in the chemical-based CPC phenomena is related to the difficulty in regulating and controlling the reaction. Microbial or enzymatic hydrolysis of urea can be one of the reliable options to control the pH, hence preferentially regulating the reaction (Ivanov et al., 2019a). Additionally, Akiyama and Kawasaki (2012) reported that relatively lower amount of CPC precipitation was occurred in pre-mixing method (~28  $\text{kg}/\text{m}^3$ ). When compared with the typical biocement (Whiffin et al., 2007), the content of precipitate was around two times lower than that reported to achieve a measurable strength in soils (threshold was ~60  $\text{kg}/\text{m}^3$ ). This indicates that a multiple supplies of calcium-phosphate stock solution are required for an effective treatment. Moreover, it has been reported that the cost of the analytical grade calcium and phosphate reagents and additives are too expensive for widespread applications (Kawasaki and Akiyama, 2013b).

The purpose of this research work is therefore to test a new eco-friendly low-cost biocement for soil improvement using calcium phosphate precipitation driven through enzymatic urea hydrolysis. Bone meal (BM) powder, one of the excellent and low-cost sources of calcium and inorganic phosphate (Makara et al., 2015), was used as cementing material instead of analytical reagents. The acid-dissolved BM, together with urea and acid urease, was injected into the sand to achieve the cementation. The utilization of bone wastes of meat processing industries for geotechnical engineering practices is indeed a novel idea; to the best of our knowledge, no existing mechanism makes use of the bone waste or employs acid urease to regulate the pH for calcium phosphate cementation. There were two major objectives: (i) demonstrating the viability of the proposed mechanism and (ii) evaluating the treatment recipes from functional, economic and environmental point of view. For that, a number of the cases were tested by varying the concentration of urea in cementation solution to evaluate the effect of urea in controlling pH. The evaluation program was based on the needle penetration tests, measurements of cement content, scanning electron microscopy (SEM), energy dispersive spectroscopy (EDS) and X-ray diffraction (XRD) analyses. While discussing the results, the economic and environmental advantages of this proposed method are also outlined.

### 1.1. Significance

The method proposed and investigated in this study is a cleaner approach, offering numerous economic and ecological benefits compared to typical biocementation methods. The method showed a new direction to sustainably make the use of bone waste (from food industries) for geotechnical engineering purposes, thus controlling the generation and accumulation of the waste. Due to the utilization of waste as cementing resources, the method could substantially reduce the cost and make it more feasible to large-scale applications. More importantly, the method could solve the long-existed problem in typical biocement methods, which is the emission of toxic ammonia gas. Since the treatment pH is well regulated in a range between acidic to neutral conditions, it could significantly eliminate the release of toxic gaseous ammonia to the atmosphere (over 90%). Moreover, the optimum recipe of cementation grout is systematically identified herein, promoting the

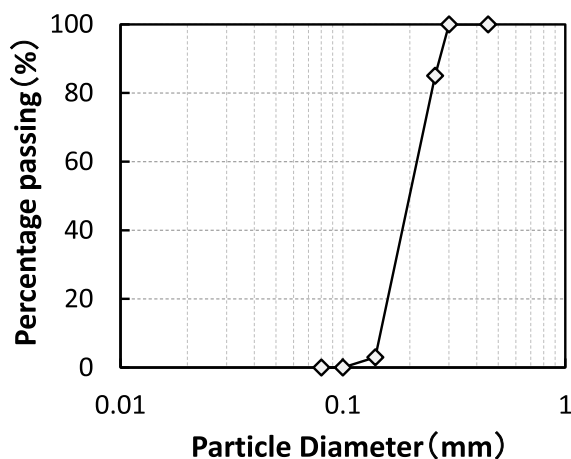


Fig. 2. Grain size distribution curve of sand used in this study.

method to be readily adopted for real-scale applications.

## 2. Materials and methods

### 2.1. Sand used

The soil used in this research work was a commercially available sand (Toyoura sand, Japan). Toyoura sand is a clean silica sand, chemically stable and has been previously used in many biocement investigations (Gowthaman et al., 2019a; Kawasaki and Akiyama, 2013b). The particle size distribution curve of the sand is shown in Fig. 2. According to the Unified Soil Classification System (USCS) (ASTM, 2017), the sand can be classified as poorly graded fine sand, having a mean particle diameter ( $D_{50}$ ) of 0.2 mm, particle density ( $\rho_s$ ) of 2.64 g/cm<sup>3</sup>, minimum density ( $\rho_{min}$ ) of 1.335 ± 0.005 g/cm<sup>3</sup>, maximum density ( $\rho_{max}$ ) of 1.645 ± 0.010 g/cm<sup>3</sup>, maximum void ratio ( $e_{max}$ ) of 0.973 and minimum void ratio ( $e_{min}$ ) of 0.609.

### 2.2. Bone meal, acid urease and preparation of biocementing solution

Commercially available BM powder, purchased from Tamagoya Company, Ibaraki, Japan, was used in this study. According to the manufacturer's specifications, the BM powder was produced by fine crushing the steamed bones of cow. Fig. 3 presents the results of X-ray diffraction analysis (the testing method is explained in subsequent

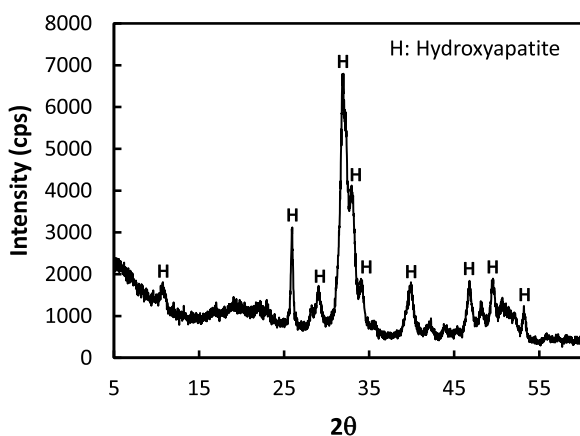


Fig. 3. The mineral composition of BM powder (obtained from XRD analysis using MultiFlex-Rigaku, Tokyo, Japan).

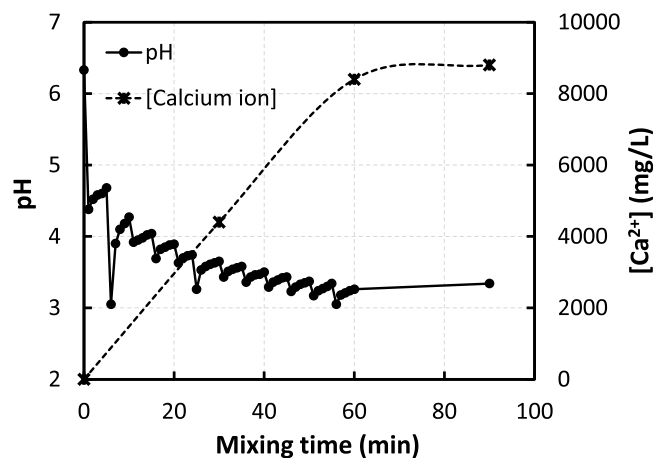
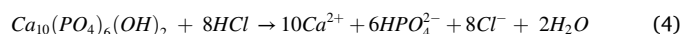


Fig. 4. The pH and Ca<sup>2+</sup> concentrations during the dissolution of bone meal powder in concentrated hydrochloric acid.

section), indicating that the calcium (Ca) and phosphate (P) in BM occur as hydroxyapatite (Ca<sub>10</sub>(PO<sub>4</sub>)<sub>6</sub>(OH)<sub>2</sub>) at Ca/P molar ratio of 1.67.

To produce the BM solution, 50 g of BM powder and 2 M HCl were added into 0.2 L of distilled water (while kept at stirring). The HCl was added in a rate of 0.005 L per every 5 min (to the total HCl addition of 0.06 L), and meanwhile, the pH and Ca<sup>2+</sup> concentrations were measured in the solution. The dissolution of BM powder (hydroxyapatite of the bone) is shown in Eq. (4). The measurements (Fig. 4) indicated that the pH of the BM solution significantly dropped with the increasing addition of HCl. Concurrently, owing to the dissolution of BM (i.e. hydroxyapatite), the concentration of calcium ions increased. After 90 min (i.e., when the measurements showed negligible changes with the time), undissolved BM residues were filtered and eliminated from the solution. The final concentration (Ca<sup>2+</sup>) and pH of the BM solution were 8800 mg/L and 3.4, respectively.



The acid urease (Product name: *Nagapshin*) used herein was supplied by Nagase Chemtex Corporation (Kyoto, Japan). The enzymatic activity of the acid urease at varying pH levels were evaluated using indophenol spectrophotometry (Bolleter et al., 1961), and the measurements are shown in Fig. 5. Relatively higher activity could be seen at acidic range

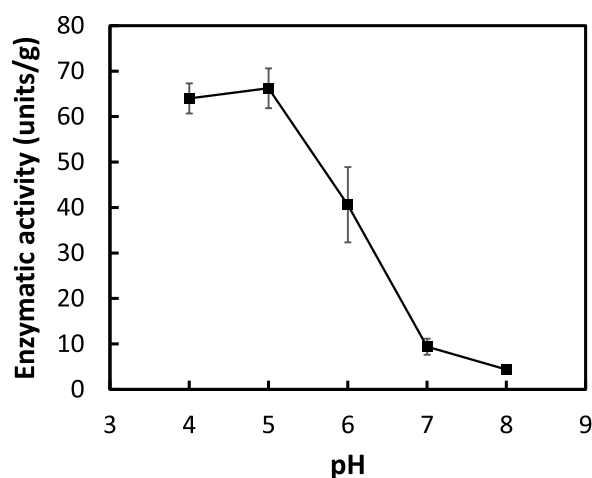


Fig. 5. The enzymatic activity of acid urease used in this study. The activity was measured within the pH range of 4.0–8.0, and the vertical error bars represent the mean ± SD (n = 3).

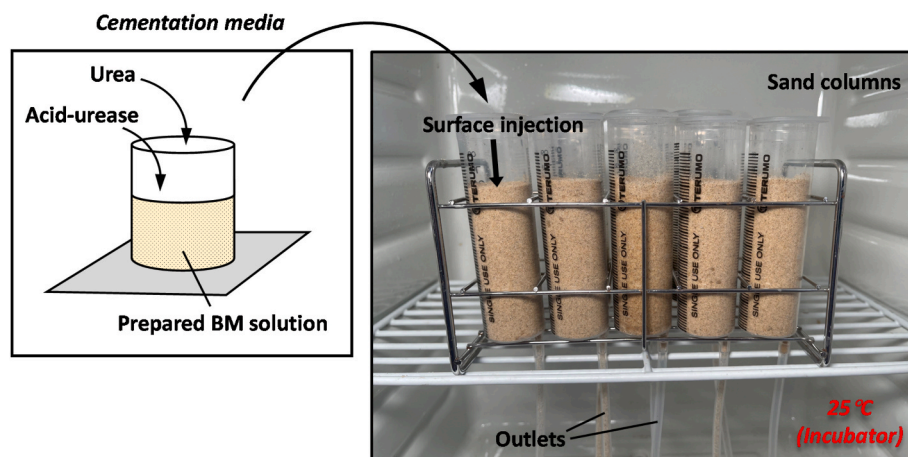


Fig. 6. The experimental set up of sand specimens prepared using syringe columns.

(pH 4.0–5.0), suggested that the urease can be effectively applied to hydrolyze urea at acidic pH.

### 2.3. Biocementation process and testing

The biocementation solution consisted of three following components: (i) acid extract of BM, (ii) acid urease and (iii) urea (as graphically illustrated in Fig. 6). Acid urease was dissolved in the prepared BM solution to the concentration of 4 g/L with urease activity of 2.5 mM/min at pH 4.0. It should be noted that relatively similar concentration of urease with urease activity of 4.5 mM/min at pH 7.0 was also used effectively in many previous works (Almajed et al., 2019; Jiang et al., 2016). In this study, different concentrations of urea were used to prepare different cementation solutions, and the testing cases, summarized in Table 1, are differentiated by the ratio between the molar concentration of  $\text{Ca}^{2+}$  and urea, herein after indicated as  $[\text{Ca}]/[\text{urea}]$  molar ratio. As summarized in Table 1, the  $[\text{Ca}]/[\text{urea}]$  ratio was varied from 0.25 to 6 to investigate the appropriate range for an effective biocementation process.

The sand was packed in vertically positioned syringe columns (30 mm in diameter and 70 mm in height) to the average dry density in the range of  $1.5 \pm 0.05 \text{ g/cm}^3$ . The experimental setup is illustrated in Fig. 6. In total, nine sand columns were prepared for the treatment using different cementation solutions (corresponding to the cases listed in Table 1). As recommended in many previous works (Cheng et al., 2019; Gowthaman et al., 2019b; Omoregie et al., 2019), the biocementation medium was injected at the top of the column at the rate of 10 mL/min and let to percolate through the sand under gravitational and capillary forces. Injection (20 mL per injection) was performed to the columns

every 24 h-basis, until ensuring the clogging effect in soil (targeted number of injections was 20). Following each injection, the percolated solutions were collected at the outlets of syringe columns and subjected to following chemical analysis: (i) measurements of  $\text{Ca}^{2+}$  (using LAQUA-twin calcium meter, HORIBA Advanced Techno Co., Ltd., Japan) and (ii) pH (using LAQUA-9615S pH meter, HORIBA Advanced Co., Ltd., Japan). After the treatment process, the molds were cut, and the specimens were carefully removed from the molds. In addition, the specimens were sufficiently rinsed using distilled water prior to further experimentations, which is mainly to eliminate the unreacted/soluble chemicals and to avoid the yielding of any additional products with the time.

### 2.4. Unconfined compression test

The unconfined compressive strength (UCS) of the cemented specimens was determined using needle penetration test (SH-70, Maruto Testing Machine Company, Tokyo) according to the standard of Japanese Geotechnical Society (JGS, 2012). The needle penetration test is the widely used method for reliable evaluating the UCS of the biocemented soil specimens (Danjo and Kawasaki, 2016; Fukue et al., 2011; Nawarathna et al., 2018). During the measurement, cemented specimen was laterally positioned, and the needle attached to the device was subjected to the penetration into the specimen. Simultaneously, the penetration resistance (measured in N) and depth of the penetration (measured in mm) were obtained from the penetrometer scale. Using the developed regression relationship, the unconfined compressive strength of the specimen was estimated.

### 2.5. Determination of the biocement content

The cement content was evaluated by acid reaction method (Fukue et al., 1999). In this method, a simplified device was used to react the cemented sample with concentrated HCl in a closed system. Firstly, the oven-dried ( $105^\circ\text{C}$  for 48 h) biocemented soil sample of known mass was placed into the device. Secondly, vials filled with sufficient quantity of 2M HCl were carefully placed into the device without contacting the sample. By trembling the device, the reaction between sample and HCl was enabled within the closed system. The digital manometer fabricated with the system was used to monitor the internal pressure variations during the reaction. The acid-reacted sand was then washed well with distilled water and oven-dried ( $105^\circ\text{C}$  for 48 h). Since the calcium compounds are inherently soluble in concentrated acid, the total mass of the cementation could be evaluated by the difference between the dry mass of the sand before and after acid-reaction (Eq. (5)). Similar phenomenon was also used in many previous works (Cui et al., 2020;

**Table 1**  
Cementation solutions prepared for different testing cases.

Case No.	Initial pH	Concentration of acid urease (g/L)	Concentration of $\text{Ca}^{2+}$ (g/L)	Concentration of urea (g/L)	Molar ratio $[\text{Ca}^{2+}]/[\text{urea}]$
1	3.4	4.0	8.8	35.20	0.25
2	3.4	4.0	8.8	8.80	1.0
3	3.4	4.0	8.8	5.87	1.5
4	3.4	4.0	8.8	4.40	2.0
5	3.4	4.0	8.8	2.93	3.0
6	3.4	4.0	8.8	2.20	4.0
7	3.4	4.0	8.8	1.47	6.0
8	3.4	4.0	8.8	0.00	–

Note: The cementation solution was prepared (shortly before percolation through the sand) by dissolution of acid urease and urea in prepared BM solution. Case 8 is the control, wherein the urea was not added.

Gowthaman et al., 2021; Neupane et al., 2015). Using Eq. (6), total cementation content (%) was computed as the ratio between total mass of the cementation and mass of untreated sand. As explained in previous section, CPCs would be anticipated to be the major cementing material; however, there would also be a possibility for minor formation of calcium carbonate (if the carbonates produced in urea hydrolysis were speciated as  $\text{CO}_3^{2-}$  in the reaction solution). From the pressure reading obtained during reaction (due to the release of  $\text{CO}_2$  gas), mass of the existed  $\text{CaCO}_3$  was evaluated, hence the content of  $\text{CaCO}_3$  was estimated using the Eq. (7). Besides, as per the Eq. (8), the calcium phosphate content was determined by subtracting the  $\text{CaCO}_3$  content from the total cementation content.

$$\text{Mass of total cementation} = \text{Dry mass before acid reaction} - \text{Dry mass after acid reaction} \quad (5)$$

$$\text{Total cementation content (\%)} = \frac{\text{Mass of total cementation}}{\text{Dry mass before acid reaction} - \text{Mass of total cementation}} \quad (6)$$

$$\text{CaCO}_3 \text{ content (\%)} = \frac{\text{Estimated mass of CaCO}_3}{\text{Dry mass before acid reaction} - \text{Mass of total cementation}} \quad (7)$$

$$\text{Calcium phosphate content (\%)} = \text{Total cementation content (\%)} - \text{CaCO}_3 \text{ content (\%)} \quad (8)$$

## 2.6. SEM, EDS and XRD

After the UCS testing, representative samples were collected (from each testing case), dried (at  $60^\circ$  for 48 h) and preserved for SEM, EDS and XRD analyses. The SEM-EDS was conducted using energy dispersive X-ray fluorescence spectrometer with SEM (JSM-IT200(JEOL), Tokyo, Japan) at an accelerating voltage of 15 kV. Before subjected to the analysis, the preserved segments were coated using carbon coater (EC-32010CC(JEOL), Tokyo, Japan). XRD analysis was carried out using the diffractometer (MultiFlex-Rigaku, Tokyo, Japan) equipped with  $\text{CuK}\alpha$  X-ray source (operating at 40 kV and 40 mA). The testing was performed to powdered samples at a scan rate of  $6.5^\circ/\text{min}$  and at angles from  $5^\circ$  to  $70^\circ$  ( $2\theta$ ). All the results obtained in this work are presented and extensively discussed in subsequent section.

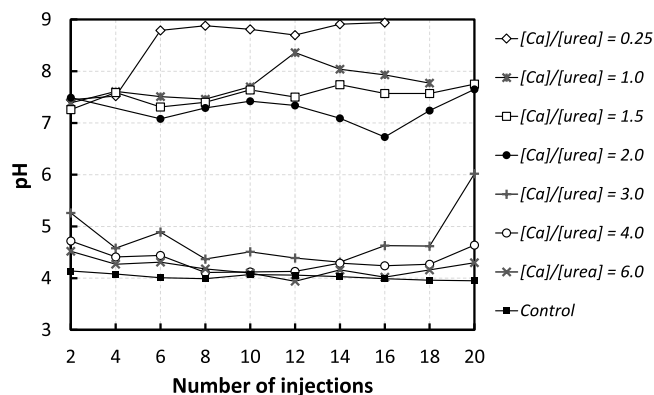


Fig. 7. The pH in effluent of the specimens treated by cementation solution with different  $[\text{Ca}]/[\text{urea}]$  molar ratios.

## 3. Results and discussion

### 3.1. Observations during the treatment

During the treatment, the reaction extent was monitored indirectly by measuring the pH and  $\text{Ca}^{2+}$  of samples collected as column effluent. In all cases, the cementation medium was introduced to the soil at the pH around 3.6; however, the outlet measurements (Fig. 7) indicated considerable escalation in pH ranging between 4.0 and 9.0, depending on the test case. This upsurge of pH could mainly be attributed to the dissolution of ammonium produced during urea hydrolysis by acid-urease (Martinez et al., 2013). It is further revealed that the quantity of added urea greatly

influenced in determining final pH of the reaction medium. For the treatment by  $[\text{Ca}]/[\text{urea}]$  ratio of 0.25 (Case 1), the outlet pH showed an increase up to  $8.5 \pm 0.5$ , whereas, it showed an increase to only around  $4.1 \pm 0.2$  for the  $[\text{Ca}]/[\text{urea}]$  of 4.0 (Case 6), suggesting that the increase in urea content increase the extent of reaction pH.

Fig. 8 shows the profile of  $\text{Ca}^{2+}$  concentration in column effluent. As seen, for the  $[\text{Ca}]/[\text{urea}]$  ratios of 0.25 and 1 (Cases 1 and 2), effluent concentrations were pretty low throughout the treatment, indicated high utilization of  $\text{Ca}^{2+}$  (over 90%) for crystallization. However, with further increase in  $[\text{Ca}]/[\text{urea}]$  ratio, the utilization of  $\text{Ca}^{2+}$  reveals a decreasing tendency, and that is likely to be in an inverse relationship with outlet pH. For instance, when the  $[\text{Ca}]/[\text{urea}]$  ratio was increased to 6.0 (Case 7), the average utilization of  $\text{Ca}^{2+}$  reduced to around 7% (which is around 13 times lower compared to Case 1). In control specimen with no urea content (Case 8), all the injected  $\text{Ca}^{2+}$  were leached out without being utilized. It is very evident that the concentration of urea in cementation solution regulates the utilization of  $\text{Ca}^{2+}$  ions, which is mainly because of the upsurge of pH (via urea hydrolysis) that decreases the solubility of CPCs. Depending on the extent of upsurge, the solubility of calcium phosphate declined, thus the ions got crystallized

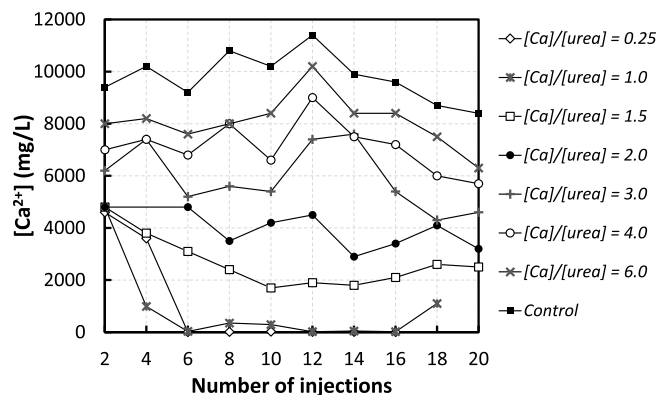


Fig. 8. The concentrations of  $\text{Ca}^{2+}$  ions in effluent of specimens treated by cementation solution of varying  $[\text{Ca}]/[\text{urea}]$  ratios.

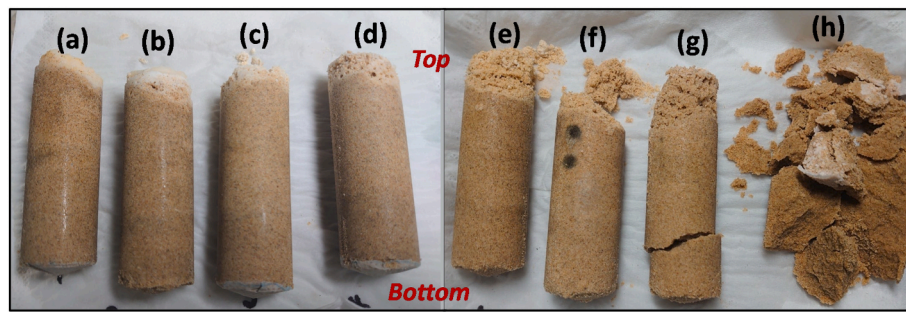


Fig. 9. The physical appearance of the specimens of different testing cases: (a)  $[Ca]/[urea] = 0.25$  (Case 1), (b)  $[Ca]/[urea] = 1.0$  (Case 2), (c)  $[Ca]/[urea] = 1.5$  (Case 3), (d)  $[Ca]/[urea] = 2.0$  (Case 4), (e)  $[Ca]/[urea] = 3.0$  (Case 5), (f)  $[Ca]/[urea] = 4.0$  (Case 6), (g)  $[Ca]/[urea] = 6.0$  (Case 7) and (h) control (Case 8).

within pore spaces of the sand.

During the treatment, it was also noticeable that the percolation rate of injected solutions appeared to decrease with increasing number of cementation injections in almost all the testing cases (except the control). It was more salient in the Cases 1 and 2, when the  $[Ca]/[urea]$  molar ratio was 0.25 and 1, respectively. The specimens got clogged by the end of sixteen and eighteen number of injections, respectively in Cases 1 and 2, thus further penetration of solution onto the soil was unachievable in the both cases. On the other hand, as planned, injections were continued until twenty-numbers in other cases (Cases 2–8).

### 3.2. Strength and uniformity of biocementation

Following the treatment process, the specimens were flushed with distilled water and prepared for the strength measurements. Fig. 9 presents the appearance of the treated specimens. The observation indicated that the soil particles were cemented throughout the column in all the testing cases (except the control case). As expected, the control specimen was not solidified, which remained similar to the untreated loose sand. Fig. 10 shows the results of needle penetration tests carried out to the columns treated using cementation solution with different  $[Ca]/[urea]$  ratios. From the results, two things can be observed: (i) the UCS of the columns decreases with the increase of  $[Ca]/[urea]$  ratio, and (ii) the UCS decreases with column depth in all the tested cases. Although the number injections performed during the treatment were low for  $[Ca]/[urea]$  ratio of 0.25 (Case 1), it exhibited the highest estimated UCS ( $1.62 \pm 0.396$  MPa). On the other hand, the UCS was measurable only around the top zone for  $[Ca]/[urea]$  ratio of 3 (Case 5), while the specimen bottom remained very weak. When the columns were treated using  $[Ca]/[urea]$  ratios of 4.0 and 6.0 (Case 6 and 7), measurable increase in strength was not achieved all over the specimens.

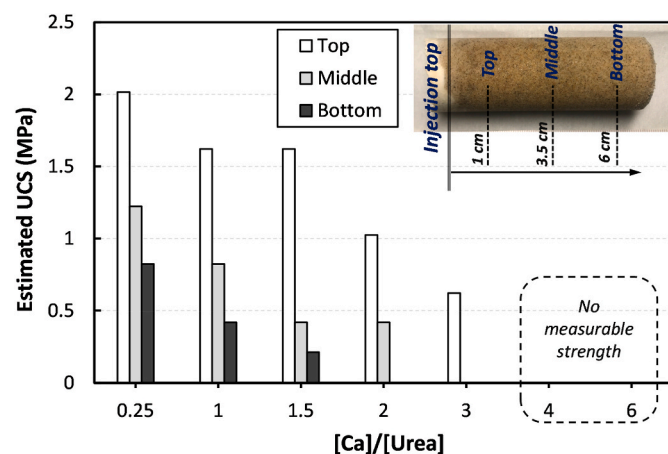


Fig. 10. Comparison of the UCS of specimens estimated by the needle penetration test.

Using small-scale columns, the consolidation was shown to achieve to the depth of 70 mm for the fine sand. In fact, the depth of consolidation is influenced by number of factors including particle size distribution, porosity and methods of treatment (Cheng and Cord-Ruwisch, 2014; Chung et al., 2020). Particle size distribution and porosity influences the flow dynamics. Owing to low infiltration capacity, the soils with less porosity (e.g., fine-grained or well-graded) reveal high risk of surface clogging. In traditional techniques, mixing is known to be effective for cementing greater depths (DeJong et al., 2006). For non-destructive cementations, high infiltration rate of solutions is preferred to achieve consolidation to a greater depth in soils. For instance, Cheng and Cord-Ruwisch (2014) showed that for the rates of 0.25 cm/min and 18 cm/min, 10% and 80% unreacted solutions were respectively reached to the bottom, indicated that movement of solution is essential to be controlled to supply the resources to depths. Despite varying factors, the effective consolidation depth seems to be determined herein by  $[Ca]/[urea]$  ratio.

It is worthwhile mentioning that the heterogeneity in cementation pattern is a general problem in biocementation method when it is performed by the percolation through a surface (Cheng and Cord-Ruwisch, 2014; Lin et al., 2016; Zamani et al., 2019). Therefore, to address the uniformity, a quantitative evaluation on precipitation is essential. Following the strength measurements, the specimens were cut into sections, and precipitation contents were measured at three different depths of the columns (1 cm, 3.5 cm, and 6 cm). Fig. 11 shows the spatial variation of biocement content. The cementing agent was non-uniformly distributed along the depth. The biocement content near the column top was higher compared to that of bottom in almost all the cases. This heterogeneity can be explained by the clogging effect during injection. In fact, the formation of calcium phosphate starts taking place as soon as the urea is mixed with biocementation medium. During repeated injections, the precipitates clogged sand and is accumulated near the sand

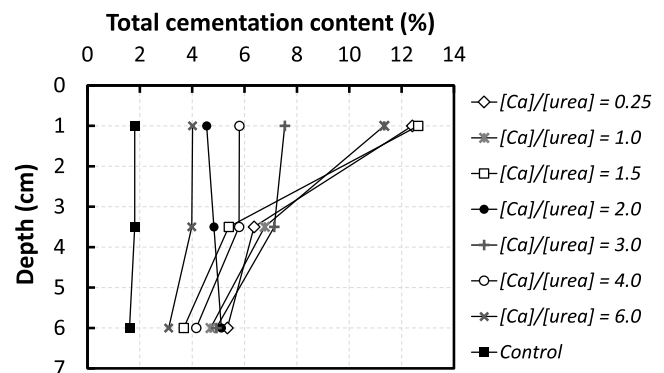


Fig. 11. The spatial distribution of biocement content in specimens after different testing cases.

surface. Similar clogging phenomena by premature formation of crystals upon early inoculation of urease with cementation solution was witnessed in previous biocement treatments as well (He et al., 2020; Mahawish et al., 2018). The occurrence of clogging was further verified by the color transformation (to white) observed around the column surface (refer to Fig. 9).

Although the clogging rapidly contributes to the development of high surface strength via increased crystals and reduced porosity, it impedes the free flow of subsequent biocement solution into the sand matrix (Omoregie et al., 2019). Concentration of biocementation medium is one of the most important factors that determine the rate of crystallization and associated clogging (Cheng et al., 2016; Omoregie et al., 2019; Tang et al., 2020). In this study, the clogging effect and heterogeneity were much more pronounced for the cases of low [Ca]/[urea] ratios (Fig. 11). The treatment homogeneity enhanced with increasing of [Ca]/[urea] ratio. This indicates that the urea concentration must be kept at possible minimum level in the cementation medium for an effective application. Using low activity solution can be another possible way to prevent the clogging effect (Chu et al., 2014). Due to the low rate of crystal formation, the pores might remain open for a prolonged period and permit the transmission of cementation medium, possibly resulting in a uniform cementation along the depth. Rather the surficial injections, pre-mixing can be effective in terms of the treatment uniformity; however, only one time treatment may be possible in pre-mixing, hence the cementation might have weaker bonding strength (Jiang and Soga, 2017). Further studies, therefore, should focus on achieving uniform cementation that is desirable in Geotechnical applications.

The average quantities of precipitates in each testing case are plotted in Fig. 12. Although the CPCs were the major precipitation component in all cases, a minor precipitation of calcium carbonate was also evidenced. In particular, the cases of low [Ca]/[urea] ratios showed comparatively high  $\text{CaCO}_3$  content. The highest formation of  $\text{CaCO}_3$  ( $1.35 \pm 0.73\%$ ) was achieved in [Ca]/[urea] ratio of 0.25 (Case 1), while it turned out to be insignificant when the added urea concentration decreased. It is clear that the  $\text{CO}_3^{2-}$  involved in  $\text{CaCO}_3$  precipitation was produced from hydrolysis of urea. However, worth mentioning that the proportion of total carbonate that speciates as  $\text{CO}_3^{2-}$  in the solution is dependent on the pH (Jacob, 1999). When the urea content was high in cementation solution (Cases 1–2), the reaction pH eminently exceeded 7.5 (refer the outlet pH measurements in Fig. 7). This slightly alkaline environment created a

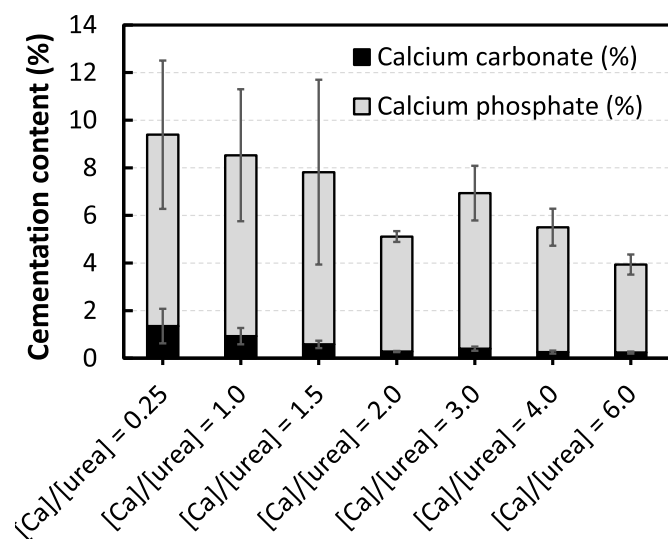


Fig. 12. The average precipitation contents of calcium phosphate and calcium carbonate in treated specimens.

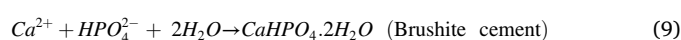
condition to the speciation of  $\text{HCO}_3^-$ , thus resulted in certain precipitation of  $\text{CaCO}_3$  from unstable  $\text{Ca}(\text{HCO}_3)_2$ . Instead, the precipitated carbonate content was negligible in other cases (Cases 4–7), which is possibly because of the dominant speciation of carbonic acid at acidic or neutral pH.

### 3.3. Characteristics of precipitation

To assess the variation in cemented microstructure, the SEM analysis was performed with the sand treated using different biocementation solution (i.e., at different [Ca]/[urea] ratios), and the images are compared in Fig. 13. For the treatment using [Ca]/[urea] ratio of 0.25 (Fig. 13(a)), a well cemented microstructure is seen, in which the precipitates were formed both at particle-particle contact points and on grain surface. However, topography of the precipitates shows an irregular amorphous-like structure, i.e., the typical crystalline structures of CPCs were not detected anywhere in the matrix. Fig. 13(b) indicates, when the [Ca]/[urea] ratio of cementation solution was 1.0, the crystal morphology of precipitates showed a combination of amorphous-like, plate-like and petal-like structures. The petal-like crystallization seemed to be occurred due to the growth of plate-like crystals in multiple directions from the same point. A bulk formation of regular plate-like crystals (25–40  $\mu\text{m}$ ) was witnessed in sand treated using [Ca]/[urea] ratio of 1.5 (Fig. 13(c)). In this case, there was no secondary formation of crystals. It should be noted that with further increase in [Ca]/[urea] ratio (particularly above 2.0), the morphology of the crystals showed dominant needle-like structures (as seen in Fig. 13(d–e)). The needle-like formation observed herein is in consistent with the formation reported by Akiyama and Kawasaki (2012) when the chemicals were mixed to produce calcium phosphate cement. Fig. 13(f) depicts the micrograph of control case. Although there some loose net-like formations were seen on the surface of the sand grains, but the sand particles remained uncemented.

The SEM images with EDS analysis depicted in Fig. 14 show the distribution of phosphate (P), calcium (Ca) and silica (Si) in cases with different [Ca]/[urea] ratio. During the analysis, the distributions of Ca and P, as the proxy of calcium phosphate, were detected, and the Si analysis distinguish the sand particles. As per the spectrum highlights, the distribution of Ca was precisely comparable with that of P in all the cases, indicating that sand particles were cemented with calcium phosphate crystals. The results further elucidate that the quantity of precipitated calcium phosphate decreased with the increase of [Ca]/[urea] ratio of biocementation medium, corroborating the propensity observed in the measured cement content discussed in previous section (Fig. 12).

The XRD spectra shown in Fig. 15 demonstrate that irrespective of the cases, the CPC that precipitated during the treatment is brushite produced during the process presented in Eq. (9). In consideration of SEM (Fig. 13), EDS (Fig. 14) and XRD (Fig. 15) results, two major differences were observed between the cases: (i) morphology and (ii) content of brushite. Firstly, the morphologies of the brushite precipitated at different [Ca]/[urea] ratio are different. As unveiled in Table 2, the amorphous-like brushites were formed in the cases with low [Ca]/[urea] (Cases 1–2), while the needle-like brushites were prominent at high [Ca]/[urea] (Cases 5–7). As reported by Toshima et al. (2014), the brushite morphology in aqueous solution is controlled by several factors such as initial concentration of calcium/phosphate, initial pH and pH changes. Since the initial concentrations and pH were kept identical in all the tested cases (Cases 1–7), the discrepancy observed in morphology could be attributed to the varying pH. The weaker needle-like brushites were formed at the marginal increase in pH (for [Ca]/[urea] 3.0–6.0), thus the cementation was not be as effective at improving the mechanical properties of the sand (refer to the UCS results presented in Fig. 10).



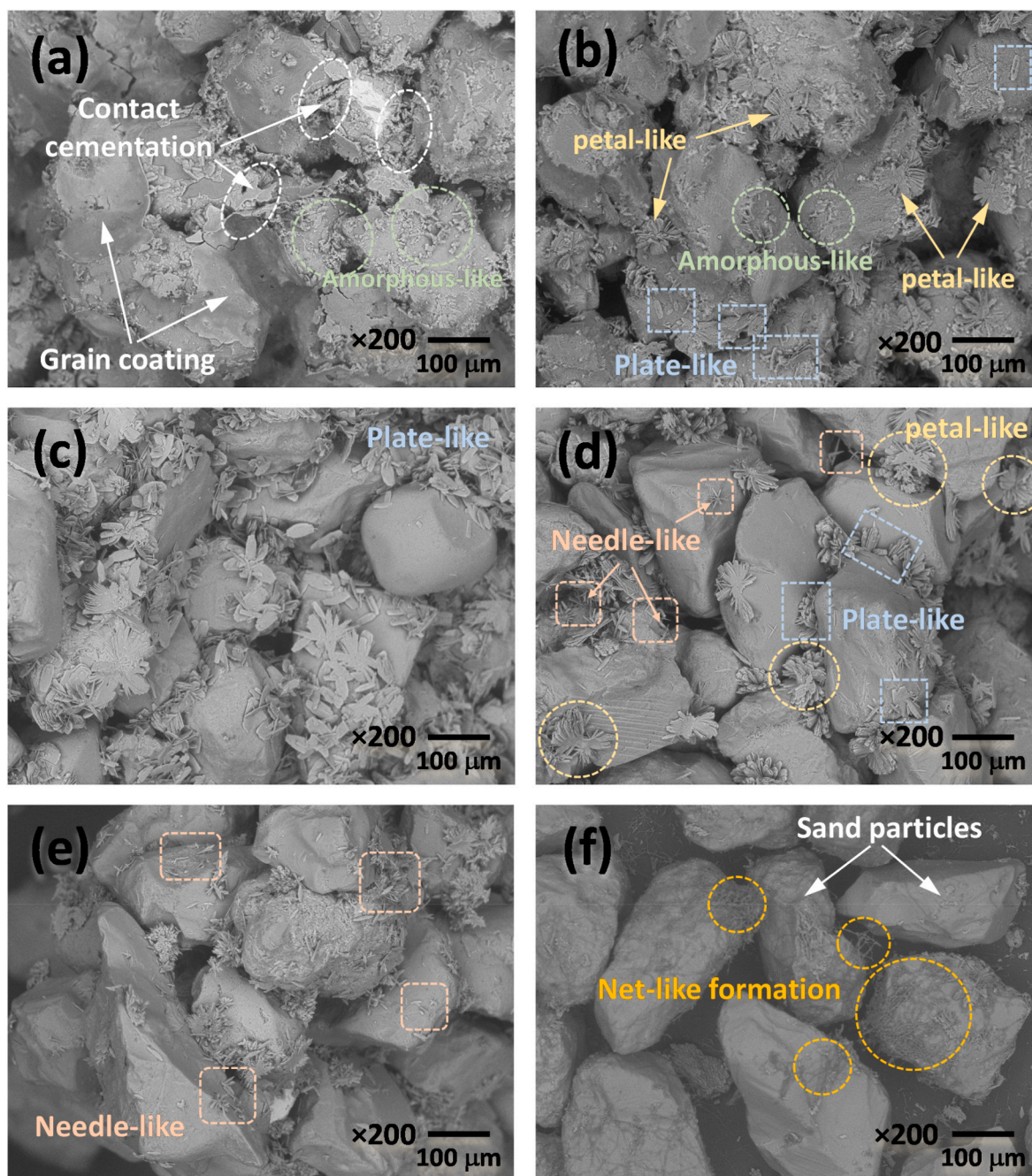


**Fig. 13.** The SEM images of the treated sand matrix for the (a)  $[\text{Ca}]/[\text{urea}] = 0.25$  (Case 1), (b)  $[\text{Ca}]/[\text{urea}] = 1.0$  (Case 2), (c)  $[\text{Ca}]/[\text{urea}] = 1.5$  (Case 3), (d)  $[\text{Ca}]/[\text{urea}] = 2.0$  (Case 4), (e)  $[\text{Ca}]/[\text{urea}] = 4.0$  (Case 6) and (f) control (Case 8).

The typical and the most stable morphology of the brushite is plate-like (i.e., tabular) crystals (Chen et al., 2017; He et al., 2011). Among the varying tested cases, the plate-like formation was progressed only in sand matrix treated using cementation solution with  $[\text{Ca}]/[\text{urea}]$  of 1.0–2.0 (Table 2). To be specific, regular plate-like crystals without any secondary formations are conspicuous for  $[\text{Ca}]/[\text{urea}]$  of 1.5. A possible explanation is that the lowermost solubility of brushite is in the pH range between 7.0 and 8.0, thus providing ideal condition for its crystallization (Kohn et al., 2002; Tung, 1998). As the reaction pH of the above-mentioned cases befell in that preferred range, the plate-like crystals were preferentially formed.

The formation of more stable polymorph is indispensable to achieve a higher binding strength in the clusters (Gebauer et al., 2008; Tamimi et al., 2012). During the treatment, the brushite crystals tended to coat

the soil particles and to cement them at particle-particle contact points. As per the previous works, the peak strength could be attributed to the contact cementation that predominantly facilitate the cohesion, while the residual strength could be from the frictional parameter (Cui et al., 2017; Gowthaman et al., 2020). Tang et al. (2020) reported that the larger clusters are responsible for stronger interparticle connections. For  $[\text{Ca}]/[\text{urea}]$  of 1.0–2.0, the plate-like crystals that are inherently larger in size, appeared to facilitate effective interparticle bridges, hence high peak strength and cohesion can be expected. The localization of crystals on grain surfaces is more likely contributing to effective interlocking, thus high residual strength and friction angle can also be expected. On the other hand, amorphous are known to be the weakest and smallest morphology of the minerals (Wang et al., 2019). However, in the case of  $[\text{Ca}]/[\text{urea}]$  ratio of 0.25, the strength was more likely to be

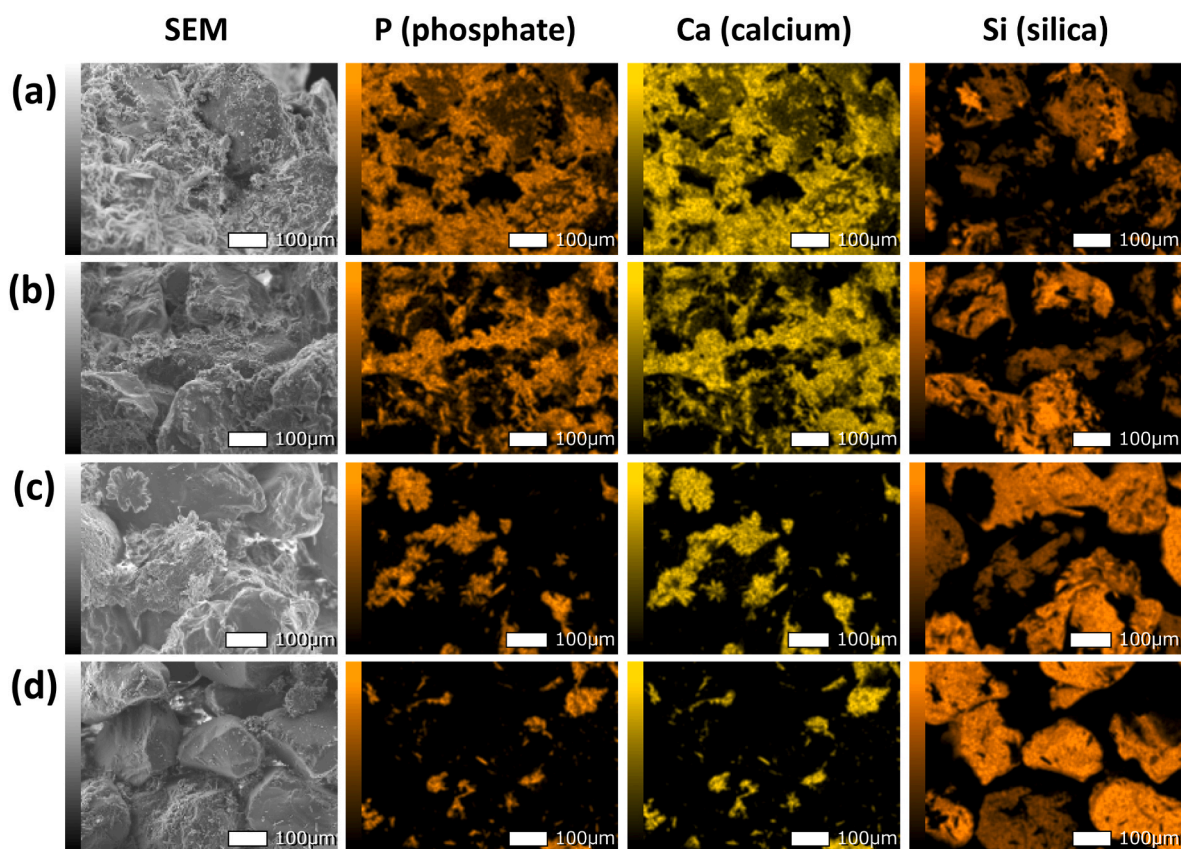


Fig. 14. The SEM-EDS analysis (for P, Ca and Si) for the sand treated in (a)  $[Ca]/[urea] = 0.25$  (Case 1), (b)  $[Ca]/[urea] = 1.5$  (Case 3), (c)  $[Ca]/[urea] = 2.0$  (Case 4) and (d)  $[Ca]/[urea] = 4.0$  (Case 6).

compensated by the increased quantity of precipitation, rather the strength or size of the binding crystals.

### 3.4. Cost analysis

The feasibility of the technique does not depend only on technical aspects, but also accompany with economic challenges. One of the greatest hurdles in achieving the complete feasibility of most of the existing biocementation techniques is the material cost (Achal et al., 2009; Mujah et al., 2017). The cost of the reagents/materials required for typical biocementation process takes over around 60% of the total operation cost (Kristiansen, 2006), which is indeed expensive especially when implicated at field-scales. To clearly reveal the economic feasibility of the proposed method, a detailed cost analysis was performed and compared with the typical MICP/EICP-based biocement (Table 3). It should be mentioned that the presented costs are based on the market price procured in Japan, and which may vary from country to country. In typical MICP/EICP biocement, calcium chloride is used as the source of calcium, and the costs of technical-grade and analytical-grade chemicals are around 150 JPY (US\$ 1.5) and 5600 JPY (US\$ 53) per kilogram, respectively. The commercial BM powder (steamed and pre-treated) that is used in the proposed method is costing around 350 JPY (US\$ 3.3) per kilogram in the market. Worth mentioning that it would be even cheaper if the BM is acquired from the food waste. Bone wastes can possibly be obtained from the restaurants, meat-processing industries, etc. for low costs without any pre-treatments and are readily applicable for producing cementation medium.

The cementation solution of the typical MICP/EICP biocement entails high urea concentration, which is typically in a range between 0.5 and 1 M (equivalent to 30–60 g/L) (Almajed et al., 2019; Putra et al., 2020). Instead, a lesser quantity of urea is required in the proposed

method. Considering the cementation solution corresponding to  $[Ca]/[urea]$  of 1.5, around 0.1 M urea concentration (equivalent to 6 g of urea/L) was evidently adequate to achieve the desirable pH level and effective cementation. This suggests that the required urea dosage for CPC biocement can be reduced by 5–10 times compared to the conventional MICP/EICP biocement. Moreover, the market price of alcali-tolerant urease used in typical EICP is extremely expensive, more than 25 times higher compared to that of the acid urease used in this work. It should be noted, however, the use of crude urease (e.g.: plant extracts) in the place of acid/alcali-tolerant urease may further reduce the cost.

The calculated cost for the 1 L of CPC biocementation solution by the proposed method is around 2210 JPY (US\$ 21), while the cost of the typical EICP biocementation solution is about 30,020 JPY/L (US\$ 285/L) (refer to Table 3). The cost difference of 14-fold discloses that the proposed CPC biocement can be remarkably affordable in industrial-scale applications. One thing should be mentioned that the cost of the proposed method can further be reduced, if the commercial acid urease can be replaced by the acid-tolerant urease-producing bacteria (Ivanov et al., 2019a). According to the previous reports, the estimated cost of the growth medium required for bacteria cultivation ranges between 28 and 880 JPY (US\$ 0.27–8.4) per 1 L (Gowthaman et al., 2019b; Omoriegbe et al., 2017), which is considerably lower than that costed herein for acid urease, 1500 JPY (US\$ 14.3). However, before involving the acid-tolerant urease-producing bacteria (instead of acid urease), two things must be carefully considered: (i) endurance and (ii) bio-safety. For instance, the most popular bacteria that can effectively produce urease under acidic environment are *Helicobacter pylori* (Bauerfeind et al., 1997); however, they are highly pathogenic. One potential candidate can be urease-producing lactic acid bacteria that are tolerable in acidic environment, such as *Lactobacillus reuteri* and *Lactobacillus fermentum* (Suzuki et al., 1979). Since these species are used in foods including

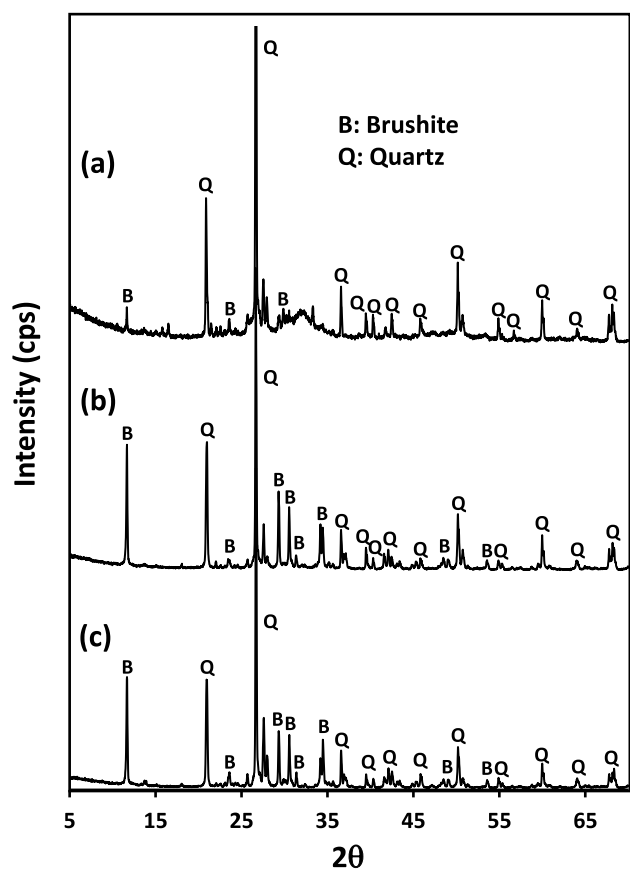


Fig. 15. The XRD analysis for the test cases of (a)  $[Ca]/[urea] = 0.25$  (Case 1), (b)  $[Ca]/[urea] = 1.5$  (Case 3) and (c)  $[Ca]/[urea] = 4.0$  (Case 6).

**Table 2**  
Summary of the precipitation characteristics of different testing cases.

Case No.	$[Ca^{2+}]/[urea]$ molar ratio of cementation solution	Range of pH increase	Precipitation type (from XRD)	Crystal morphology (from SEM)
1	0.25	3.4 → 8.5 ± 0.5	Brushite	Amorphous-like
2	1.0	3.4 → 7.7 ± 0.2	Brushite	Amorphous-like, plate-like
3	1.5	3.4 → 7.5 ± 0.1	Brushite	Plate-like
4	2.0	3.4 → 7.0 ± 0.5	Brushite	Plate-like, needle-like
5	3.0	3.4 → 4.9 ± 0.9	Brushite	needle-like
6	4.0	3.4 → 4.1 ± 0.2	Brushite	needle-like
7	6.0	3.4 → 4.0 ± 0.0	Brushite	needle-like

yogurt, probiotics, fermented milk, cheese production, etc., they are safer and more likely to be approved for geotechnical applications.

### 3.5. Environmental benefit

There are two major environmental benefits in the proposed CPC method over typical MICP/EICP biocement method: (i) reduced formation of total ammonium, and (ii) eliminating the formation of toxic ammonia gas. It is well known that the ammonium by-products are environmentally detrimental (Ivanov et al., 2019a; van Paassen et al.,

2010). The stoichiometry of urea hydrolysis (given in Eq. (1)) indicates that the production of total ammonium can be twice of the urea concentration. As mentioned earlier, the typical MICP/EICP biocementations are performed at molar  $[Ca]/[urea]$  ratio from 0.66 to 1.0. Meanwhile, the proposed CPC method is attained at a  $[Ca]/[urea]$  molar ratio of 1.5, indicating that the total production of ammonium during biocementation process can be potentially decreased by around 50%. As reported by Ivanov et al. (2019b), around 22 kg of ammonium is produced in typical MICP/EICP biocementation of 1 m<sup>3</sup> sand. Therefore, the proposed CPC biocement is more likely than typical MICP/EICP biocement to get approved for large-scale applications.

Another significance of this method is the potential to eliminate the emission of gaseous ammonia. In typical MICP/EICP biocement, around 5.8 g gaseous ammonia is emitted per the injection of 1 L cementation solution (Yu et al., 2020). The fact is that the emission of gaseous ammonia is more difficult and uncontrollable than dealing with ionic forms that can possibly be treated at the effluents (Lee et al., 2019; Mohsenzadeh et al., 2021). Fig. 16 clearly elucidates that the emission can be controlled by desirably amending the recipe of cementation medium. For the  $[Ca]/[urea]$  of 0.25 (Case 1), the reaction pH was heeded up to 9.0 [which is comparable with the pH increase in typical biocements (Martinez et al., 2013; Naveed et al., 2020)], indicating discharge of gaseous ammonia up to 36.5% of produced total. However, with the increase in  $[Ca]/[urea]$  ratio in cementation solution, the desirable pH ranges are achieved (Fig. 16). When the  $[Ca]/[urea]$  ratio exceeds 1.0, the liberation of gaseous ammonia appears to be substantially controlled, revealing a decrease by over 90% compared to typical MICP/EICP biocements.

## 4. Potential applications and limitations

The obtained findings suggest that different  $[calcium]/[urea]$  ratios of cementation solution can result in different functional, economic and environmental efficacies. Worth saying, to choose the better recipe for cementation solution, the considerations must collectively be taken into account. The ability to acquire high effective strength with less consumed chemicals and less harmful by-products, is highly desirable for any engineering practices. Functional-wise, low  $[calcium]/[urea]$  ratio can be preferred, i.e.,  $[calcium]/[urea] = 0.25-2.0$ . On the other hand, high  $[calcium]/[urea]$  ratio may reduce both the material cost and environmental damage, i.e.,  $[calcium]/[urea] = 1.0-$  and above. The optimal  $[calcium]/[urea]$  ratio, therefore, appears to fall in the range between 1.0 and 2.0, and which is recommended for the real-scale applications.

For stabilizing ground, transportation subgrades and embankments, an adequate strength needs to be achieved by producing sufficient calcium phosphate bonds between soil grains. The UCS achieved in proposed approach can be comparable with those of conventional biocementation methods (MICP/EICP), immensely satisfying typical threshold requirements of pavement subgrade treatment and liquefaction control (Duraisamy, 2016; Islam et al., 2020), potentially at low-cost and in an environmentally-friendly manner. The study further demonstrated that the treatment could desirably transition the loose sand to a rock-like material with extremely high aggregate stability, indicating a wide range of other possible applications such as erosion control, slope preservation, near-surface stabilization and coastal protection. It should be noted, however, the proposed biocement did not reach the required strength properties of industrial cement (i.e., OPC) which has two orders magnitude compressive strength, thus cannot be feasible/recommended for building and construction industries.

How the bone-based cement compete with the industrial demand, is a major concern in the proposed method. It is well known that the industrial cement demand is currently over 5 billion tons, while the global slaughter industry produces only 130 million ton of animal bone residues every year. One thing is clear that the demand of the industrial cement cannot be entirely fulfilled by the proposed calcium phosphate

**Table 3**

Detailed cost comparison between the cementation solutions of proposed CPC method and typical EICP biocementation method.

Proposed CPC biocementation method (mediated by acid urease)				Typical EICP biocementation method (mediated by alcalitolerant urease)			
Required substances	<sup>a</sup> Unit price	<sup>b</sup> Required quantity	Cost	Required substances	<sup>a</sup> Unit price	Required quantity	Cost
Bone meal	350 (JPY/kg)	190 (g/L)	66.5 (JPY)	Calcium chloride	<sup>d</sup> 150 (JPY/kg)	<sup>c</sup> 55.5–111 (g/L)	8.3–16.7 (JPY)
Urea	<sup>d</sup> 170 (JPY/kg)	5.87 (g/L)	1.0 (JPY)	Urea	<sup>d</sup> 170 (JPY/kg)	<sup>c</sup> 30–60 (g/L)	5.1–10.2 (JPY)
Acid urease	375,000 (JPY/kg)	4 (g/L)	1,500 (JPY)	Alcalitolerant Urease	10,000,000 (JPY/kg)	<sup>c</sup> 3 (g/L)	30,000 (JPY)
Hydrochloric acid	2,800 (JPY/L)	0.23 (L/L)	644 (JPY)				
Total cost (per L cementation solution)			2,210 JPY (US\$ 21)	Total cost (per L cementation solution)			30,020 JPY (US\$ 285)

<sup>a</sup> The presented costs are based on the market price of Japan (which may vary from country to country).

<sup>b</sup> The calculated quantities are based on the Case 3 ([Ca]/[urea] ratio of 1.5).

<sup>c</sup> Given ranges of calcium chloride, urea and urease are based on the previous biocementation research (Almajed et al., 2019; Jiang et al., 2016).

<sup>d</sup> The presented costs of urea and calcium chloride are corresponding to technical-grade.

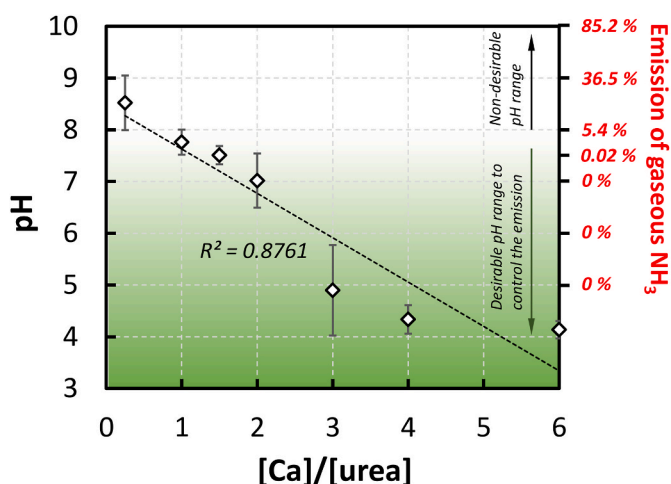


**Fig. 16.** The mean effluent pH plotted against [Ca]/[urea] ratio, along with the interpretation of gaseous ammonia emission in the tested cases with respect to their pH condition.

cement; however, it can partly replace the production of OPC, thus contributing to the minimization of global carbon dioxide emission. Since the production of 1 ton Portland cement emits around 0.81 ton of CO<sub>2</sub> gas (Benhelal et al., 2012), even a certain replacement of OPC in geotechnical industry by bone-based biocement would be greatly beneficial from the sustainable point of view.

## 5. Conclusions

In this study, a new eco-friendly CPC biocementation was proposed and demonstrated in the laboratory scale for soil improvement purpose. The strategy involved the pH-dependent mechanism to precipitate the calcium phosphate by urea hydrolysis process that increases the pH from acidic to neutral level. Injecting cementation solution that consisted of acid-dissolved BM, urea and acid-urease was shown to result in the formation of insoluble calcium phosphate cement to bind the soil particles together. The pH increase during reaction could be effectively controlled by the content of urea in cementation solution i.e., [calcium]/[urea] ratios. The outcomes indicated that the pH increase had a great influence on (i) the precipitation quantity of calcium phosphate and (ii) the morphology of the formed crystals, indicating that the emphasis should be given on effectively choosing the quantity of urea in the CPC cementation solution. XRD analysis revealed that the formed crystals were found to be brushite, regardless of the [calcium]/[urea] ratios. However, [calcium]/[urea] ratio of 1.5 in cementation solution resulted in preferable formation of plate-like crystals within the sand matrix and increased unconfined compressive strength up to 1.5 MPa.

Comparing with conventional biocements, the proposed method offers enormous economic and ecological advantages. The proposed method showed a new direction to sustainably utilize the bone waste for soil improvement purpose, thus controlling the generation and accumulation of the waste. The cost analysis showed that the material cost of the treatment was reduced by around fourteen-times compared to the conventional biocement. Moreover, since the treatment pH can be easily controlled at or below neutral conditions (3.4–7.5), it can substantially eliminate the release of toxic gaseous ammonia to the atmosphere (over 90% in comparison with conventional biocementations). With these significant findings, further studies are encouraged for promoting this ecofriendly approach towards the field implementations.

## Data availability statement

All the experimental data that support the findings of this study are available from the corresponding author upon reasonable request through email.

## CRediT authorship contribution statement

**Sivakumar Gowthaman:** designed the experimental program, performed laboratory experiments and wrote the manuscript. **Moeka Yamamoto:** performed the laboratory experiments and analyzed the testing results. **Kazunori Nakashima:** supported in data analysis, interpretations and reviewed the manuscript. **Volodymyr Ivanov:** supported in data interpretations and reviewed the manuscript. **Satoru Kawasaki:** contributed primary supervision, reviewed and approved it for publication. All the authors listed have made direct and intellectual contribution to the presented work.

## Declaration of competing interest

The authors declare that they have no known competing financial interests or personal relationships that could have appeared to influence the work reported in this paper.

## Acknowledgements

This research work was partially supported by JSPS KAKENHI, grant number JP19H02229, Japan, and by the funding of the Japan Society for the Promotion of Science (JSPS), FY2019JSPS Invitational Fellowships for Research in Japan (Short-term) ID S19124. The authors gratefully acknowledge the support.

## References

Achal, V., Mukherjee, A., Basu, P.C., Reddy, M.S., 2009. Lactose mother liquor as an alternative nutrient source for microbial concrete production by *Sporosarcina*

- pasteurii*. J. Ind. Microbiol. Biotechnol. 36, 433–438. <https://doi.org/10.1007/s10295-008-0514-7>.
- Achal, V., Mukherjee, A., Kumari, D., Zhang, Q., 2015. Biomineralization for sustainable construction - a review of processes and applications. Earth Sci. Rev. 148, 1–17. <https://doi.org/10.1016/j.earscirev.2015.05.008>.
- Akiyama, M., Kawasaki, S., 2012. Novel grout material comprised of calcium phosphate compounds: in vitro evaluation of crystal precipitation and strength reinforcement. Eng. Geol. 125, 119–128. <https://doi.org/10.1016/j.enggeo.2011.11.011>.
- Almajed, A., Abbas, H., Arab, M., Alsabhan, A., Hamid, W., Al-Salloum, Y., 2020. Enzyme-induced carbonate precipitation (EICP)-based methods for ecofriendly stabilization of different types of natural sands. J. Clean. Prod. 274, 122627 <https://doi.org/10.1016/j.jclepro.2020.122627>.
- Almajed, A., Tirkolaei, H.K., Kavazanjian, E., Hamdan, N., 2019. Enzyme induced biocemented sand with high strength at low carbonate content. Sci. Rep. 9, 1135. <https://doi.org/10.1038/s41598-018-38361-1>.
- ASTM, 2017. Standard Practice for Classification of Soils for Engineering Purposes (Unified Soil Classification System). American Society for Testing and Materials, West Conshohocken, PA.
- Bauerfeind, P., Garner, R., Dunn, B.E., Mobley, H.L.T., 1997. Synthesis and activity of *Helicobacter pylori* urease and catalase at low pH. Gut 40, 25–30. <https://doi.org/10.1136/gut.40.1.25>.
- Benhelal, E., Zahedi, G., Hashim, H., 2012. A novel design for green and economical cement manufacturing. J. Clean. Prod. 22, 60–66. <https://doi.org/10.1016/j.jclepro.2011.09.019>.
- Bolleter, W.T., Bushman, C.J., Tidwell, P.W., 1961. Spectrophotometric determination of ammonia as indophenol. Anal. Chem. 33, 592–594. <https://doi.org/10.1021/ac60172a034>.
- Chen, Y., Shen, C., Rashid, S., Li, S., Ali, B.A., Liu, J., 2017. Biopolymer-induced morphology control of brushite for enhanced defluorination of drinking water. J. Colloid Interface Sci. 491, 207–215. <https://doi.org/10.1016/j.jcis.2016.12.032>.
- Cheng, L., Cord-Ruwisch, R., 2014. Upscaling Effects of soil improvement by microbially induced calcite precipitation by surface percolation. Geomicrobiol. J. 31, 396–406. <https://doi.org/10.1080/01490451.2013.836579>.
- Cheng, L., Shahin, M.A., Chu, J., 2019. Soil bio-cementation using a new one-phase low-pH injection method. Acta Geotech 14, 615–626. <https://doi.org/10.1007/s11440-018-0738-2>.
- Cheng, L., Shahin, M.A., Mujah, D., 2016. Influence of key environmental conditions on microbially induced cementation for soil stabilization. J. Geotech. Geoenviron. Eng. 143, 04016083 [https://doi.org/10.1061/\(asce\)gt.1943-5606.0001586](https://doi.org/10.1061/(asce)gt.1943-5606.0001586).
- Chu, J., Ivanov, V., Naeimi, M., Stabnikov, V., Liu, H.L., 2014. Optimization of calcium-based bioclogging and biocementation of sand. Acta Geotechnica 9, 277–285. <https://doi.org/10.1007/s11440-013-0278-8>.
- Chung, H., Kim, S.H., Nam, K., 2020. Application of microbially induced calcite precipitation to prevent soil loss by rainfall: effect of particle size and organic matter content. J. Soils Sediments. <https://doi.org/10.1007/s11368-020-02757-2>.
- Cui, M.-J., Lai, H.-J., Hoang, T., Chu, J., 2020. One-phase-low-pH enzyme induced carbonate precipitation (EICP) method for soil improvement. Acta Geotechnica. <https://doi.org/10.1007/s11440-020-01043-2>.
- Cui, M.-J., Zheng, J.J., Zhang, R.J., Lai, H.J., Zhang, J., 2017. Influence of cementation level on the strength behaviour of bio-cemented sand. Acta Geotechnica 12, 971–986. <https://doi.org/10.1007/s11440-017-0574-9>.
- Danjo, T., Kawasaki, S., 2016. Microbially induced sand cementation method using *Pararhodobacter* sp. strain SO1, inspired by beachrock formation mechanism. Mater. Trans. 57, 428–437. <https://doi.org/10.2320/matertrans.M-M2015842>.
- DeJong, J.T., Fritzsche, M.B., Nüsslein, Klaus, 2006. Microbially induced cementation to control sand response to undrained shear. J. Geotech. Geoenviron. Eng. 132 (11), 1381–1392. [https://doi.org/10.1061/\(ASCE\)1090-0241\(2006\)132:11\(1381\)](https://doi.org/10.1061/(ASCE)1090-0241(2006)132:11(1381)).
- DeJong, J.T., Mortensen, B.M., Martinez, B.C., Nelson, D.C., 2010. Bio-mediated soil improvement. Ecol. Eng. 36, 197–210. <https://doi.org/10.1016/j.ecoleng.2008.12.029>.
- Duraisamy, Y., 2016. Strength and Stiffness Improvement of Bio-Cemented Sydney Sand. Doctoral Dissertation. University of Sydney, Australia.
- Fukue, M., Nakamura, T., Kato, Y., 1999. Cementation of soils due to calcium carbonate. Soils Found. 39, 55–64. <https://doi.org/10.3208/sandf.39.6.55>.
- Fukue, M., Ono, S.-I., Sato, Y., 2011. Cementation of sands due to microbially-induced carbonate precipitation. Soils Found. 51, 83–93. <https://doi.org/10.3208/sandf.51.83>.
- Gebauer, D., Völkel, A., Cölfen, H., 2008. Stable prenucleation calcium carbonate clusters. Science 322 (5909), 1819–1822. <https://doi.org/10.1126/science.1164271>.
- Ginebra, M.P., Fernández, E., De Maeyer, E.A.P., Verbeeck, R.M.H., Boltong, M.G., Ginebra, J., Driessens, F.C.M., Planell, J.A., 1997. Setting reaction and hardening of an apatitic calcium phosphate cement. J. Dent. Res. 76, 905–912. <https://doi.org/10.1177/00220345970760041201>.
- Gowthaman, S., Iki, T., Nakashima, K., Ebina, K., Kawasaki, S., 2019a. Feasibility study for slope soil stabilization by microbial induced carbonate precipitation (MICP) using indigenous bacteria isolated from cold subarctic region. SN Appl. Sci. 1, 1480. <https://doi.org/10.1007/s42452-019-1508-y>.
- Gowthaman, S., Mitsuyama, S., Nakashima, K., Komatsu, M., Kawasaki, S., 2019b. Biogeotechnical approach for slope soil stabilization using locally isolated bacteria and inexpensive low-grade chemicals: a feasibility study on Hokkaido expressway soil. Japan. Soils Found. 59, 484–499. <https://doi.org/10.1016/j.sandf.2018.12.010>.
- Gowthaman, S., Nakashima, K., Kawasaki, S., 2020. Freeze-thaw durability and shear responses of cemented slope soil treated by microbial induced carbonate precipitation. Soils Found. 60, 840–855. <https://doi.org/10.1016/j.sandf.2020.05.012>.
- Gowthaman, S., Nakashima, K., Kawasaki, S., 2021. Durability analysis of bio-cemented slope soil under the exposure of acid rain. J. Soils Sediments 21, 2831–2844. <https://doi.org/10.1007/s11368-021-02997-w>.
- He, J., Gao, Y., Gu, Z., Chu, J., Wang, L., 2020. Characterization of crude bacterial urease for CaCO<sub>3</sub> precipitation and cementation of silty sand. J. Mater. Civ. Eng. 32, 04020071 [https://doi.org/10.1061/\(ASCE\)MT.1943-5533.0003100](https://doi.org/10.1061/(ASCE)MT.1943-5533.0003100).
- He, L.H., Yao, L., Xue, R., Sun, J., Song, R., 2011. In-situ mineralization of chitosan/calcium phosphate composite and the effect of solvent on the structure. Front. Mater. Sci. 5, 282–292. <https://doi.org/10.1007/s11706-011-0140-6>.
- Islam, M.T., Chittoori, B.C.S., Burbank, M., 2020. Evaluating the applicability of biostimulated calcium carbonate precipitation to stabilize clayey soils. J. Mater. Civ. Eng. 32, 1–11. [https://doi.org/10.1061/\(ASCE\)MT.1943-5533.0003036](https://doi.org/10.1061/(ASCE)MT.1943-5533.0003036).
- Ivanov, V., Stabnikov, V., 2017. Construction Biotechnology. Biogeochemistry, Microbiology and Biotechnology of Construction Materials and Processes. Springer Singapore, Singapore. <https://doi.org/10.1007/978-981-10-1445-1>.
- Ivanov, V., Stabnikov, V., Kawasaki, S., 2019a. Ecofriendly calcium phosphate and calcium phosphate biogroups. J. Clean. Prod. 218, 328–334. <https://doi.org/10.1016/j.jclepro.2019.01.315>.
- Ivanov, V., Stabnikov, V., Stabnikova, O., Kawasaki, S., 2019b. Environmental safety and biosafety in construction biotechnology. World J. Microbiol. Biotechnol. 35, 26. <https://doi.org/10.1007/s11274-019-2598-9>.
- Jacob, D., 1999. Geochemical Cycles. In: Introduction to Atmospheric Chemistry. Princeton University Press, pp. 87–114.
- JGS, 2012. Japanese Standards and Explanations of Geotechnical and Geoenvironmental Investigation Methods (3431-2012). Japanese Geotechnical Society, Tokyo, pp. 426–432.
- Jiang, N.-J., Soga, K., 2017. The applicability of microbially induced calcite precipitation (MICP) for internal erosion control in gravel-sand mixtures. Geotechnique 67, 42–55. <https://doi.org/10.1680/jgeot.15.P.182>.
- Jiang, N.-J., Yoshioka, H., Yamamoto, K., Soga, K., 2016. Ureolytic activities of a urease-producing bacterium and purified urease enzyme in the anoxic condition: implication for subseafloor sand production control by microbially induced carbonate precipitation (MICP). Ecol. Eng. 90, 96–104. <https://doi.org/10.1016/j.ecoleng.2016.01.073>.
- Kawasaki, S., Akiyama, M., 2013a. Effect of addition of phosphate powder on unconfined compressive strength of sand cemented with calcium phosphate compound. Mater. Trans. 54, 2079–2084. <https://doi.org/10.2320/matertrans.M-M2013827>.
- Kawasaki, S., Akiyama, M., 2013b. Enhancement of unconfined compressive strength of sand test pieces cemented with calcium phosphate compound by addition of various powders. Soils Found. 53, 966–976. <https://doi.org/10.1016/j.sandf.2013.10.013>.
- Keykha, H.A., Asadi, A., 2017. Solar powered electro-bio-stabilization of soil with ammonium pollution prevention system. Adv. Civ. Eng. Mater. 6, 20170001 <https://doi.org/10.1520/ACEM20170001>.
- Keykha, H.A., Mohamadzadeh, H., Asadi, A., Kawasaki, S., 2019. Ammonium-free carbonate-producing bacteria as an ecofriendly soil biostabilizer. Geotech. Test J. 42, 20170353 <https://doi.org/10.1520/GTJ20170353>.
- Kohn, M.J., Rakovan, J.F., Hughes, J.M., 2002. Phosphates: Geochemical, Geobiological and Materials Importance (Reviews in Mineralogy & Geochemistry). The Mineralogical Society of America, Washington, DC 20036, USA.
- Kristiansen, Bjørn, 2006. Process Economics. In: Ratledge, C., Kristiansen, Bjørn (Eds.), Basic Biotechnology, third ed. Cambridge University Press, Cambridge, pp. 271–286. <https://doi.org/10.1017/CBO9780511802409.013>.
- Lee, M., Gomez, M.G., San Pablo, A.C.M., Kolbus, C.M., Graddy, C.M.R., DeJong, J.T., Nelson, D.C., 2019. Investigating ammonium by-product removal for ureolytic bio-cementation using meter-scale experiments. Sci. Rep. 9 <https://doi.org/10.1038/s41598-019-54666-1>.
- Lin, H., Suleiman, M.T., Brown, D.G., Kavazanjian, E., 2016. Mechanical behavior of sands treated by microbially induced carbonate precipitation. J. Geotech. Geoenviron. Eng. 142, 1–13. [https://doi.org/10.1061/\(ASCE\)GT.1943-5606.0001383](https://doi.org/10.1061/(ASCE)GT.1943-5606.0001383), 04015066.
- Mahawish, A., Bouazza, A., Gates, W.P., 2018. Effect of particle size distribution on the bio-cementation of coarse aggregates. Acta Geotech 13, 1019–1025. <https://doi.org/10.1007/s11440-017-0604-7>.
- Makara, A., Kowalski, Z., Saeid, A., 2015. Treatment of wastewater from production of meat-bone meal. Open Chem 13, 1275–1285. <https://doi.org/10.1515/chem-2015-0145>.
- Martinez, B.C., DeJong, J.T., Ginn, T.R., Montoya, B.M., Barkouki, T.H., Hunt, C., Tanyu, B., Major, D., 2013. Experimental optimization of microbial-induced carbonate precipitation for soil improvement. J. Geotech. Geoenviron. Eng. 139, 587–598. [https://doi.org/10.1061/\(ASCE\)GT.1943-5606.0000787](https://doi.org/10.1061/(ASCE)GT.1943-5606.0000787).
- Mohsenzadeh, A., Aflaki, E., Gowthaman, S., Nakashima, K., Kawasaki, S., Ebadi, T., 2021. A two-stage treatment process for the management of produced ammonium by-products in ureolytic bio-cementation process. Int. J. Environ. Sci. Technol. <https://doi.org/10.1007/s13762-021-03138-z>.
- Mujah, D., Shahin, M.A., Cheng, L., 2017. State-of-the-art review of biocementation by microbially induced calcite precipitation (MICP) for soil stabilization. Geomicrobiol. J. 34, 524–537. <https://doi.org/10.1080/01490451.2016.1225866>.
- Naveed, M., Duan, J., Uddin, S., Suleman, M., Hui, Y., Li, H., 2020. Application of microbially induced calcium carbonate precipitation with urea hydrolysis to improve the mechanical properties of soil. Ecol. Eng. 153, 105885 <https://doi.org/10.1016/j.ecoleng.2020.105885>.
- Nawarathna, T.H.K., Nakashima, K., Fujita, M., Takatsu, M., Kawasaki, S., 2018. Effects of cationic polypeptide on CaCO<sub>3</sub> crystallization and sand solidification by

- microbial-induced carbonate precipitation. *ACS Sustain. Chem. Eng.* 6, 10315–10322. <https://doi.org/10.1021/acssuschemeng.8b01658>.
- Neupane, D., Yasuhara, H., Kinoshita, N., Ando, Y., 2015. Distribution of mineralized carbonate and its quantification method in enzyme mediated calcite precipitation technique. *Soils Found.* 55, 447–457. <https://doi.org/10.1016/j.sandf.2015.02.018>.
- Omoriegbe, A.I., Khoshdelnezamiha, G., Senian, N., Ong, D.E.L., Nissom, P.M., 2017. Experimental optimisation of various cultural conditions on urease activity for isolated *Sporosarcina pasteurii* strains and evaluation of their biocement potentials. *Ecol. Eng.* 109, 65–75. <https://doi.org/10.1016/j.ecoleng.2017.09.012>.
- Omoriegbe, A.I., Palombo, E.A., Nissom, P.M., 2020. Bioprecipitation of calcium carbonate mediated by ureolysis: a review. *Environ. Eng. Res.* <https://doi.org/10.4491/eer.2020.379>.
- Omoriegbe, A.I., Palombo, E.A., Ong, D.E.L., Nissom, P.M., 2019. Biocementation of sand by *Sporosarcina pasteurii* strain and technical-grade cementation reagents through surface percolation treatment method. *Construct. Build. Mater.* 228, 116828 <https://doi.org/10.1016/j.conbuildmat.2019.116828>.
- Putra, H., Yasuhara, H., Erizal, Sutoyo, Fauzan, M., 2020. Review of enzyme-induced calcite precipitation as a ground-improvement technique. *Infrastructure* 5, 66. <https://doi.org/10.3390/infrastructures5080066>.
- Suzuki, K., Benno, Y., Mitsuoka, T., Takebe, S., Kobashi, K., Hase, J., 1979. Urease producing species of intestinal anaerobes and their activities. *Appl. Environ. Microbiol.* 37, 379–382. <https://doi.org/10.1128/aem.37.3.379-382.1979>.
- Tamimi, F., Sheikh, Z., Barralet, J., 2012. Dicalcium phosphate cements: brushite and monetite. *Acta Biomater.* 8, 474–487. <https://doi.org/10.1016/j.actbio.2011.08.005>.
- Tang, C.S., Yin, L., yang, Jiang, N. jun, Zhu, C., Zeng, H., Li, H., Shi, B., 2020. Factors affecting the performance of microbial-induced carbonate precipitation (MICP) treated soil: a review. *Environ. Earth Sci.* 79, 94. <https://doi.org/10.1007/s12665-020-8840-9>.
- Toshima, T., Hamai, R., Tafu, M., Takemura, Y., Fujita, S., Chohji, T., Tanda, S., Li, S., Qin, G.W., 2014. Morphology control of brushite prepared by aqueous solution synthesis. *J. Asian Ceram. Soc.* 2, 52–56. <https://doi.org/10.1016/j.jascr.2014.01.004>.
- Tung, M.S., 1998. Calcium Phosphates: Structure, Composition, Solubility, and Stability. In: *Calcium Phosphates in Biological and Industrial Systems*. Springer US, Boston, MA, pp. 1–19. [https://doi.org/10.1007/978-1-4615-5517-9\\_1](https://doi.org/10.1007/978-1-4615-5517-9_1).
- van Paassen, L.A., Ghose, R., van der Linden, T.J.M., van der Star, W.R.L., van Loosdrecht, M.C.M., 2010. Quantifying biomediated ground improvement by ureolysis: large-scale biogROUT experiment. *J. Geotech. Geoenviron. Eng.* 136, 1721–1728. [https://doi.org/10.1061/\(ASCE\)GT.1943-5606.0000382](https://doi.org/10.1061/(ASCE)GT.1943-5606.0000382).
- Wang, Y., Soga, K., Dejong, J.T., Kabla, A.J., 2019. Microscale visualization of microbial-induced calcium carbonate precipitation processes. *J. Geotech. Geoenviron. Eng.* 145, 1–13. [https://doi.org/10.1061/\(ASCE\)GT.1943-5606.0002079](https://doi.org/10.1061/(ASCE)GT.1943-5606.0002079).
- Whiffin, V.S., 2004. *Microbial CaCO<sub>3</sub> Precipitation for the Production of Biocement*. Doctoral dissertation. Murdoch University, Australia.
- Whiffin, V.S., van Paassen, L.A., Harkes, M.P., 2007. Microbial carbonate precipitation as a soil improvement technique. *Geomicrobiol. J.* 24, 417–423. <https://doi.org/10.1080/01490450701436505>.
- Yu, X., Chu, J., Yang, Y., Qian, C., 2020. Reduction of ammonia production in the biocementation process for sand using a new biocement. *J. Clean. Prod.* 2, 124928 <https://doi.org/10.1016/j.jclepro.2020.124928>.
- Zamani, A., Montoya, B., Gabr, M., 2019. Investigating the challenges of in situ delivery of MICP in fine grain sands and silty sands. *Can. Geotech. J.* <https://doi.org/10.1139/cgj-2018-0551>.